Available online at www.sciencedirect.com
SCIENCE DIRECT®
Journal of Power Sources 115 (2003) 279–287
JOURNAL OF POWER SOURCES
www.elsevier.com/locate/jpowsour

Design and testing of a fuel-cell powered battery charging station

Zhenhua Jiang, Roger A. Dougal*
Department of Electrical Engineering, University of South Carolina, Columbia, SC 29208, USA

Received 21 October 2002; accepted 4 December 2002

Abstract

The portable fuel-cell powered battery charging station provides a good solution to recharging batteries in field applications. This paper presents the design and testing of control strategies for this system using the Virtual Test Bed (VTB). The VTB provides a unique environment to model interdisciplinary components, to rapidly prototype the control system, and to simulate complex systems. In this paper, the system design is first proposed. Both static and real-time control strategies are investigated to coordinate the power distribution among batteries. The fuel cell, battery and power electronic system are modeled in the native VTB format. The charging controller is designed and implemented in MatLab/Simulink, and then is imported to VTB for system simulation. The fuel-cell powered battery charging station is simulated under the proposed charging algorithms. The performance of each charging algorithm is analyzed.

Keywords: Battery; Charging station; Fuel cell; Simulink; VTB

1. Introduction

Rechargeable batteries such as lithium ion cells are playing an increasingly significant role in the utilization of portable electronic devices such as portable computers, cellular phones and camcorders [1]. These batteries feature small size, light weight and renewable utilization in comparison to conventional primary batteries. These advantages, however, are restricted by their limited usable time. It is then necessary to develop some kind of portable battery charging system. The fuel cell, which is emerging as one of the most promising technologies for the future power sources [2,3], may provide a good solution to powering the portable charging station that may be far away from the utility power system [4].

Both the fuel cell and lithium ion battery are strongly nonlinear, and the fuel cell has a limited power capacity [5–8]. These conditions present some difficulty for the system designer. Power converters are needed to condition the power flow and should be controlled appropriately. In order to meet the requirements to simultaneously charge multiple batteries, power converters are then connected in parallel, one for each battery pack. The initial states of charge of the various batteries may be different when they are inserted into the charger. A battery with a lower initial state of charge may require a larger charging current or otherwise a longer charging time. Therefore, the power from the fuel cell should be distributed efficiently among the batteries. The power distribution from a nonlinear and current-limited power source presents obvious difficulty for the design of control strategies. In order to reduce the development cycle and costs, it is necessary to test the possible control strategies through simulation. The Virtual Test Bed (VTB) provides a good environment to model interdisciplinary components, to rapidly prototype the control system, and to simulate complex systems. The VTB allows handling natural power flow, signal and data coupling between devices of multi-disciplines and it offers a combination of both topological and mathematical expressions in model formulation for a comprehensive and efficient modeling process. In addition, the VTB is endowed with mechanisms for importing models from several languages such as MatLab/Simulink, which was valuable during the control system design [9].

In the following, the system architecture and the control issues are first described. Both static and real-time control strategies were investigated to coordinate the power distribution among the batteries. The fuel cell, battery and power electronic system were modeled in the native VTB form. The charging controller was designed and implemented in MatLab/Simulink and then imported to VTB for system simulation. Finally, the full fuel-cell powered battery charging station was simulated as it used the proposed charging algorithms.

* Corresponding author. Tel.: +1-803-777-7890; fax: +1-803-777-8045.
E-mail address: dougal@engr.sc.edu (R.A. Dougal).

0378-7753/03/$ – see front matter
doi:10.1016/S0378-7753(02)00725-5

2. System design

In general, the battery charging station should allow multiple batteries to be charged simultaneously and it should allow any battery to be inserted or retrieved at any time. While an arbitrary number of charging channels are possible, we used here three channels, which can represent the general solution to many charging channels. Since the objective of this work was to prove out the basic power sharing algorithms, we assume here that all three batteries are always in the charger. The case that some batteries are inserted or retrieved at random times will be reported later in [10].

The block diagram of the proposed fuel-cell powered battery charging station is shown in Fig. 1, where the system parameters are also shown. A fuel cell stack, which is the power generation system, is used to charge up to three lithium ion battery packs each through a dc/dc step-down power converter (buck converter). Each battery contains four series-connected lithium ion cells. Each buck converter efficiently converts the fuel cell voltage to an appropriate lower voltage to charge the corresponding battery. By controlling the buck converters, the charging currents can be regulated. A controller is used to coordinate the power converters. The controller monitors the currents and voltages of the batteries and outputs the appropriate pulse-width modulation signals to the buck converters.

From Fig. 1, it is clear that the power from the fuel cell is distributed among three batteries, which can be expressed in Eq. (1).

$$P_{fc} = P_1 + P_2 + P_3 \tag{1}$$

where P_1, P_2, and P_3 are the power to three charging channels, respectively, and P_{fc} the power from the fuel cell.

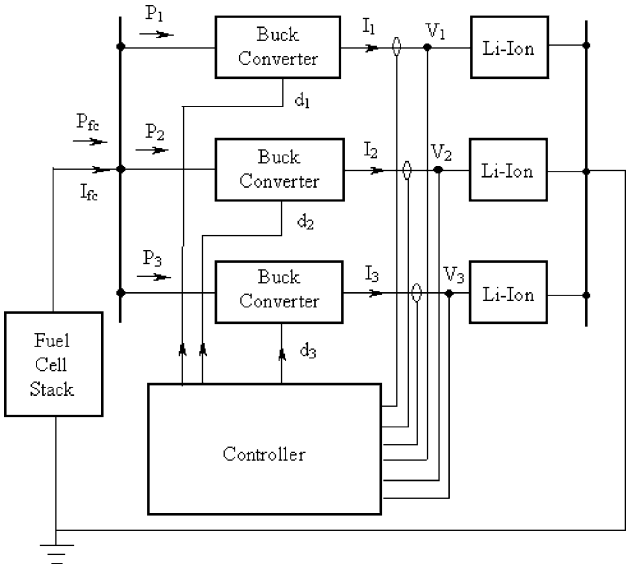

Fig. 1. Block diagram of the system design.

In practice, the power distribution among the batteries is realized by regulating the charging currents of the batteries. The following equation relates the current from the fuel cell to the three charging currents.

$$I_{fc} = d_1 I_1 + d_2 I_2 + d_3 I_3 \tag{2}$$

where I_1, I_2, and I_3 are the currents to three batteries, respectively, I_{fc} the current from the fuel cell, and d_1, d_2, d_3 the duty cycles of the three buck converters, respectively, and they have values between 0 and 1.

Since the fuel cell output current is limited, the sum of the right hand side in Eq. (2) should be less than some value (i.e. I_{max}). Considering that the variations in both the fuel cell voltage and the battery voltages are not too large, the duty cycle of the switching signal to each buck converter will vary within a limited small range (for example, from 0.7 to 0.75). Based on this assumption, we can take the following expression as a criterion for active power distribution among the batteries.

$$I_1 + I_2 + I_3 \leq I_{lim} \tag{3}$$

where I_{lim} is a preset limit for the total charging current which can be estimated according to I_{max} and the average duty cycle. Eq. (3) gives a basic requirement for the design of control strategies for active power sharing in this system.

3. Design of charging algorithm

The users may have different requirements in charging the batteries according to their own needs. While some may require that the batteries be fully charged within the shortest period of time, others may wish to charge at a slower rate in order to increase the life expectancy of their batteries. In order to discover the most appropriate control schemes for the various requirements, three charging algorithms were investigated to coordinate the power distribution among the battery branches. These strategies were equal rate charging, proportional rate charging, and pulse current charging.

Among these power sharing algorithms, Dc and pulse current charging protocols were used. dc charging protocol can help to protect the battery from overcharging. Under this protocol, the battery is charged to an end potential using a constant current. The potential is then held constant after this potential is reached, and the charging current will taper gradually. The charging process will stop when the current reaches a preset small value during the constant voltage mode. Under pulse charging protocol, a pulse current with a period of T and on-time of T_{on} is applied to the battery. Pulse current charging has been shown to enhance charging rate capability and also prevent the increase of internal impedance of the battery, thus reducing the total charging time [8].

3.1. Equal rate charging

When the initial states of charge of the batteries are close, a direct and simple approach to charging all the batteries using dc charging protocol is to distribute the charging current equally among them. Due to the small differences in the initial states of the batteries, some batteries may reach the reference voltage earlier than others. When one battery reaches its voltage limit, the voltage will be kept constant and the charging current will eventually taper to zero. The rest of the total available current will be re-distributed equally between the other batteries. Then the same scheme is followed by the remaining batteries till all batteries move to the constant voltage mode. This control strategy is illustrated in Fig. 2. This algorithm can be implemented easily but it may take a longer time for all batteries to become fully charged when the initial states of charge of the batteries are widely disparate.

3.2. Proportional rate charging

A more time-efficient method that is suitable for batteries with any initial state of charge can take into consideration the fact that the charge that the battery will need to become fully charged is the integral of the charging current over the total charging time. The depth of discharge can be used to represent a measurement of the rest of the charge. It is calculated as unity minus state of charge. If constant currents of the same magnitude are applied to charge different batteries, the charging time will be proportional to the depth of discharge (neglecting nonlinearity in the battery). On the other hand, if we want all the batteries to become fully charged at the same time, the charging current can be proportional to the fraction of the depth of discharge of each battery, which can be calculated according to Eq. (4)

$$I_i = I_{\lim} \frac{1 - \mathrm{SOC}_i}{\sum_{i=1}^{3} (1 - \mathrm{SOC}_i)}, \quad i = 1, \ldots, 3 \tag{4}$$

where I_i is the charging current of the ith battery, $I_{\lim}$ the total available charging current, and SOC_i the state of charge of the ith battery.

Although the batteries may become fully charged almost simultaneously with this algorithm, it is difficult to estimate the state of charge. For Li-ion batteries, an approximate relationship between the state of charge (SOC) and open circuit voltage can be found when the SOC is not within the extreme range, i.e. if the SOC is between 0.1 and 0.9. Therefore, the SOC can be estimated by measuring the battery voltage. In this paper, the SOC is estimated according to a linear relationship, which is given in Eq. (5).

$$\mathrm{SOC} = \frac{v_0 - a}{b} + c \tag{5}$$

where a, b and c are constants and can be easily obtained by a series of experiments, v_0 is the battery open circuit voltage which can be estimated from the following equation.

$$v = v_0 + ir \tag{6}$$

where v and i are the measured voltage and charging current of the battery, and r the equivalent series resistance of the battery.

3.3. Pulse current charging

Besides the dc charging, the third method is pulse current charging. Under this algorithm, three pulse currents with the same period of T and different on-times are applied to the batteries alternately. The sum of the on-time of each pulse is equal to the period of the pulses. The illustration of this control strategy is given in Fig. 3. A similar method as the proportional rate charging can be found for pulse charging. The duty cycles of pulse charging currents can be proportional to the fraction of the depth of discharge of each battery, which can be estimated according to the following equation.

$$D_i = \frac{1 - \mathrm{SOC}_i}{\sum_{i=1}^{3} (1 - \mathrm{SOC}_i)}, \quad i = 1, \ldots, 3 \tag{7}$$

where D_i is the duty cycle of the charging current of the ith battery,

With this algorithm, the charging current can be larger than that in the previous algorithms because only one battery is charged at any time. It is also possible for all batteries to be

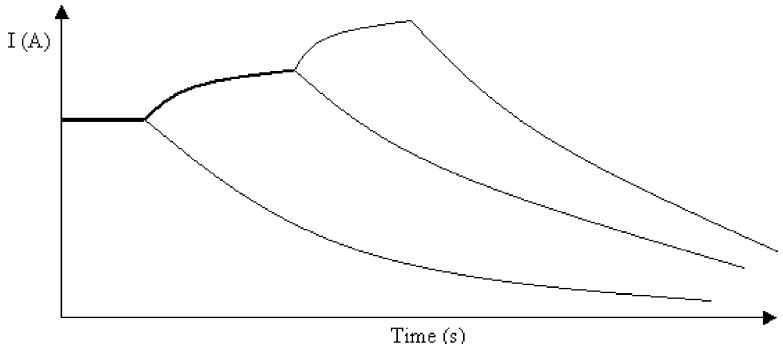

Fig. 2. Illustration of equal rate charging algorithm with three batteries each starting at different initial state of charge.

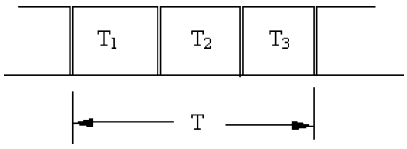

Fig. 3. Illustration of pulse current charging algorithm.

fully charged almost simultaneously; nevertheless the disadvantage is that it is difficult to implement this algorithm in the control system because it involves a lot of dynamics.

4. Component modeling

The VTB supports both native and imported model formulations: the native model is constructed using the resistive companion method [11], and the controller model implemented in Simulink can be imported to VTB. This Simulink model can be used in either of two ways. First, when the controller is still in development, the Simulink model can be used in an interactive co-simulation mode that allows adjustment of the controller parameters during system simulation. Second, once the controller design has been finalized, the controller model can be compiled into an executable that allows others to study the system behavior without having to actually run Matlab or Simulink.

The native models for the fuel cell, battery and power electronic system, as well as the VTB–Simulink interface, are available in the current version of VTB. In this section, the model description of the fuel cell, battery and power converter, and the Simulink implementation of the charging controller are described.

4.1. Fuel cell system

The electrochemical reaction process inside the fuel cell stack is very complicated. In this application, we are particularly interested in the electrical characteristics on the electrodes. The thermal transfer by the material streams is negligible. The effects of water management on the performance are neglected. The air is consumed by the fuel cell stack, and this is replaced by the consumption of the oxygen and the performance dependence on the partial pressure of the oxygen when it is mixed with nitrogen. An empirical equation given in Eq. (8) is used to describe the potential of a fuel cell stack [12].

$$V = N_{\text{cell}}\left[E_0 - b(T)\log\left(\frac{I}{A_{\text{cell}}}\right) - r(T)\frac{I}{A_{\text{cell}}} - m(P)\exp\left(n(P)\frac{I}{A_{\text{cell}}}\right)\right] \tag{8}$$

where E_0 is the standard potential of H_2–O_2 reaction, I the current from the fuel cell (mA), V the voltage of the stack (mV), N_{cell} the series number of the cells, A_{cell} the area of each cell (cm^2), T the bulk temperature of the stack (K), and P the hydrogen pressure (Pa), b and r the functions of the temperature, and m and n the functions of the pressure. The expressions for b, r, m, and n are the polynomials that are calculated empirically from the experiment data.The mass flow of the hydrogen is simply proportional to the output current and the series number of the cells, as shown below.

$$\dot{M} = N_{\text{cell}}KI \tag{9}$$

where $\dot{M}$ is the mass flow of the hydrogen, K the proportionality constant (mol/C).

The difference between the total power from the reaction and the electrical power released is the thermal power that must be expelled from the fuel cell stack. The thermal power is given by

$$Q = N_{\text{cell}}\left(\frac{\Delta H}{nF}\right)I - VI \tag{10}$$

where Q is the thermal power expelled from the fuel cell stack, ΔH the change of entropy of hydrogen, n the number of moles of hydrogen, and F the Faraday's constant.

4.2. Battery system

The objective of modeling the battery system is to replicate the electrical and thermal properties of the battery as it interacts with the external circuit. In this application, all electrochemical reactions are considered uniform throughout each porous electrode and all spatial variations of chemical concentrations and potentials are ignored. The model is obtained by fitting the data from manufacturers' data sheets or independent measurements. The equivalent electrical schematic of the model is shown in Fig. 4.

The equivalent model comprises three components: an equilibrium potential E, an internal resistance that is divided into two components R_1 and R_2, and an effective capacitance C that represents localized storage of chemical energy within the porous electrodes. The equilibrium potential of the battery depends on the temperature and the amount of active material available in the electrodes, which can be specified in terms of depth of discharge. The potential E, the

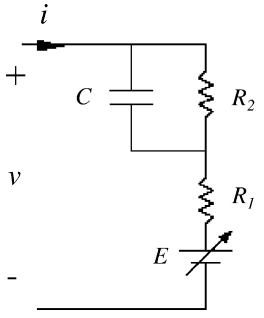

Fig. 4. Equivalent circuit of Li-ion battery based on the experimental data.

terminal voltage v and the depth of discharge DOD are related by Eqs. (11)–(13).

$$i(t) = \frac{1}{R_2}[v(t) - E[i(t), T(t), t] - R_1 i(t)] + C\frac{\mathrm{d}}{\mathrm{d}t}[v(t) - E[i(t), T(t), t] - R_1 i(t)] \quad (11)$$

$$v[i(t), T(t), t] = \sum_{j=0}^{N} c_j \mathrm{DOD}^j[i(t), T(t), t] + \Delta E[T(t)] \quad (12)$$

$$\mathrm{DOD}[i(t), T(t), t] = \frac{1}{Q_\mathrm{r}}\int_0^t \alpha[i(\tau)]\beta[T(\tau)]i(\tau)\,\mathrm{d}\tau \quad (13)$$

where i is the battery current (A), N the highest order of the fitting polynomial of the reference curve, c_j the coefficient of the jth order term in the polynomial representation, Q_r the battery capacity referred to the cut-off voltage for the reference curve (Ah), T the battery temperature (K), and t the independent time variable (s). A potential correction term $\Delta E(T)$ is used to compensate for the variation of equilibrium potential that is induced by the temperature change at the reference rate. The dependence of the depth of discharge on the rate is accounted for by a factor $\alpha(i)$. A factor $\beta(T)$ is used to account for the dependence of the depth of discharge on the temperature. The detail of how to determine these parameters can be found in [13].

The change of the battery temperature is characterized by the thermal energy balance [14] equation that is described by Eq. (14). Heat generation due to entropy change or phase change, changes in the heat capacity are ignored without apparent loss of model accuracy.

$$mc_p\frac{\mathrm{d}T(t)}{\mathrm{d}t} = i(t)^2R_1 + \frac{1}{R_2}[v(t) - E[i(t), T(t), t] - i(t)R_1]^2 - h_\mathrm{c}A[T(t) - T_\mathrm{a}] \quad (14)$$

where A is the battery external surface area (m^2), c_p the specific heat of the battery pack (J/(kg K)), h_c the heat transfer coefficient (W/(m^2 K)), m the mass of the battery (kg), and T_a is the ambient temperature (K).

4.3. Power electronic system

As mentioned before, each battery is charged by an individual buck converter. Fig. 5 shows the simplified power circuit for one of three charging channels, in which an MOSFET transistor and a power diode chop the input dc voltage to a pulse voltage, the power inductor filters the output current, and the capacitor smoothes the output voltage. The output of the buck converter is a smooth dc voltage. The power electronic system in the battery charging station is constructed by three such power converters that are connected in parallel. They have the same power source (the fuel cell) but difference loads (the batteries).

Since the goal of the system level simulation is to investigate the power balance in the fuel cell/battery system and to monitor the main parameters of the system, the simulation time step can be long, for example, higher than 1 s. In this case, a time-average model of the converter is used, and both the switching transients and the harmonic effects are neglected. The power flow in the converter is controlled by adjusting the average on/off duty cycle of the switching signal. The average output voltage of the buck converter is determined by the following equation.

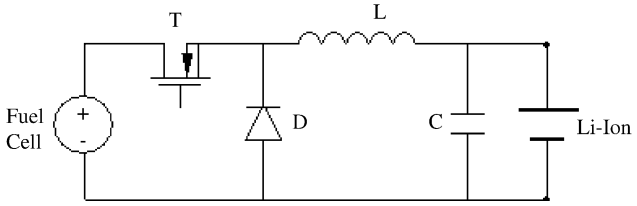

Fig. 5. Schematic of the simplified power circuit for one charging channel.

$$\frac{V_\mathrm{o}}{V_\mathrm{i}} = \frac{t_\mathrm{on}}{T} = d \quad (15)$$

where V_i and V_o are the average input and output voltages of the converter, respectively, t_on the turn-on time of the switch during a period, T the switching period, and d the average duty cycle of the switching signal.

4.4. Charging controller

Since the VTB provides a mechanism for importing models from Simulink and co-simulating with MatLab, the control algorithm can be rapidly prototyped in Simulink. The Simulink model of the charge controller is shown in Fig. 6. The voltages and charging currents of three batteries are input from VTB through six input terminals. The reference charging current for each battery and the corresponding duty cycle for each power converter are calculated in the Simulink model. The Simulink model of the controller also determines the turn-on or -off of the switch connected to each battery. The controller can output a turnoff signal when the charging stops or a fault is detected. The average values of the duty cycles and the switch states are exported to the VTB through six output terminals.

The main functional blocks in the charge controller are the charging current strategy module, the current regulation module, the voltage regulation module, and the charging termination decision module. The charging current strategy module is developed based on the proposed three power sharing algorithms. The reference charging current for each battery is calculated in this module.

The current and voltage regulation modules are used to compute the duty cycles to the buck converters according to the reference currents from the charging current strategy module and the reference voltages set up in this module, respectively. The classical proportional–integral approach is used to regulate the charging currents and voltages. The current and voltage regulation laws are formulated in

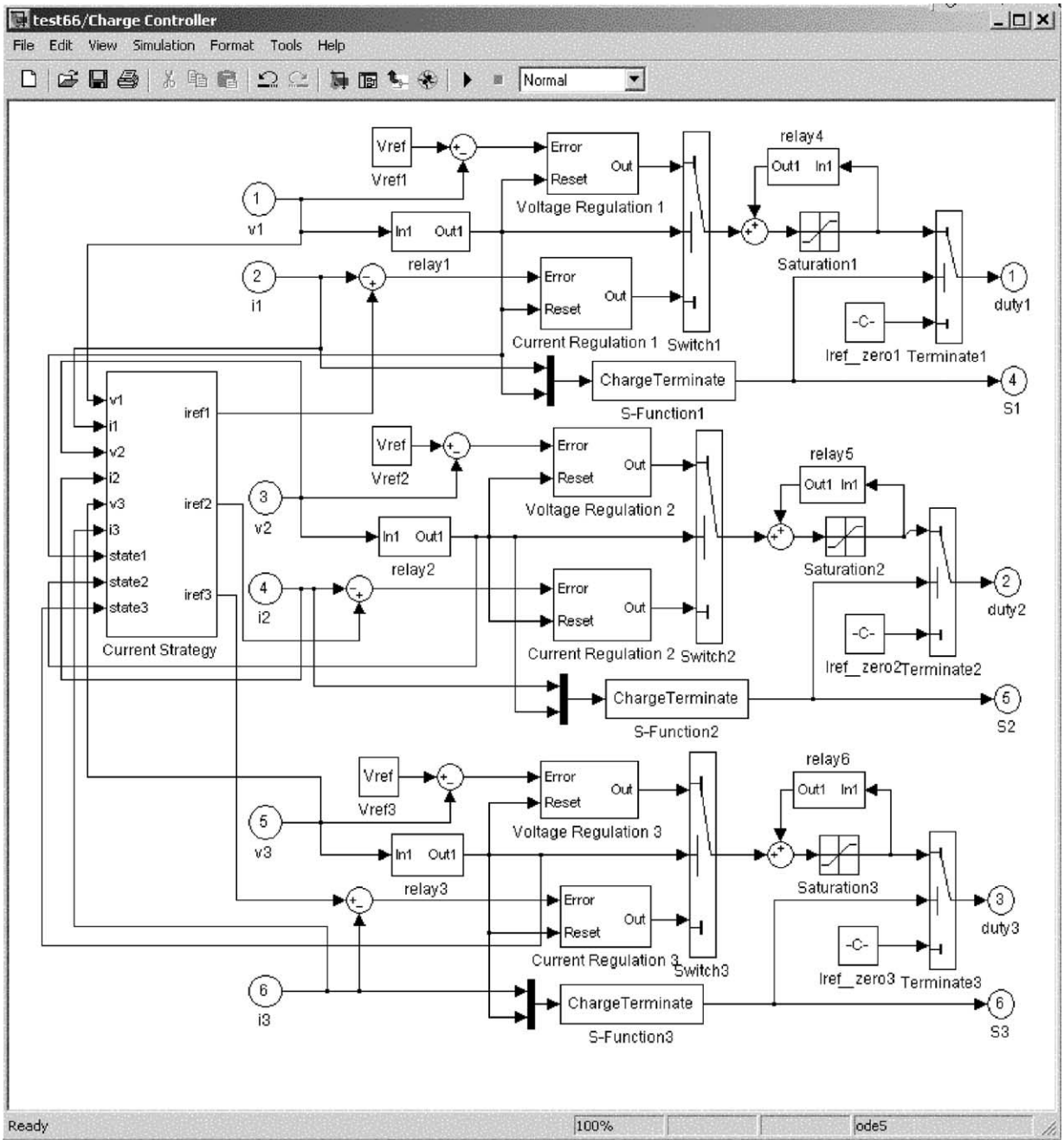

Fig. 6. Simulink model of the battery charge controller.

Eqs. (16) and (17), respectively.

$$d = d_{\text{old}} + k_{\text{pi}}(I_{\text{ref}} - I) + k_{\text{ii}} \int (I_{\text{ref}} - I)\,\mathrm{d}t \tag{16}$$

$$d = d_{\text{old}} + k_{\text{pv}}(V_{\text{ref}} - V) + k_{\text{iv}} \int (V_{\text{ref}} - V)\,\mathrm{d}t \tag{17}$$

where V, I are the measured voltage and current of the battery, d and d_{old} the current and previous duty cycles used to control the buck converter, V_{ref} and I_{ref} the reference voltage and charging current of the battery, k_{pi}, k_{ii}, and k_{pv}, k_{iv} are the proportional and integral gains for current and voltage regulations, respectively.

The charging termination decision module can determine when the charging process stops and output a turnoff signal to the corresponding power converter as the charging termination happens.

5. System simulation

In order to investigate the performance of the system together with the charge controller, the fuel-cell powered battery charging station was assembled in the VTB and the simulation study was conducted under three proposed

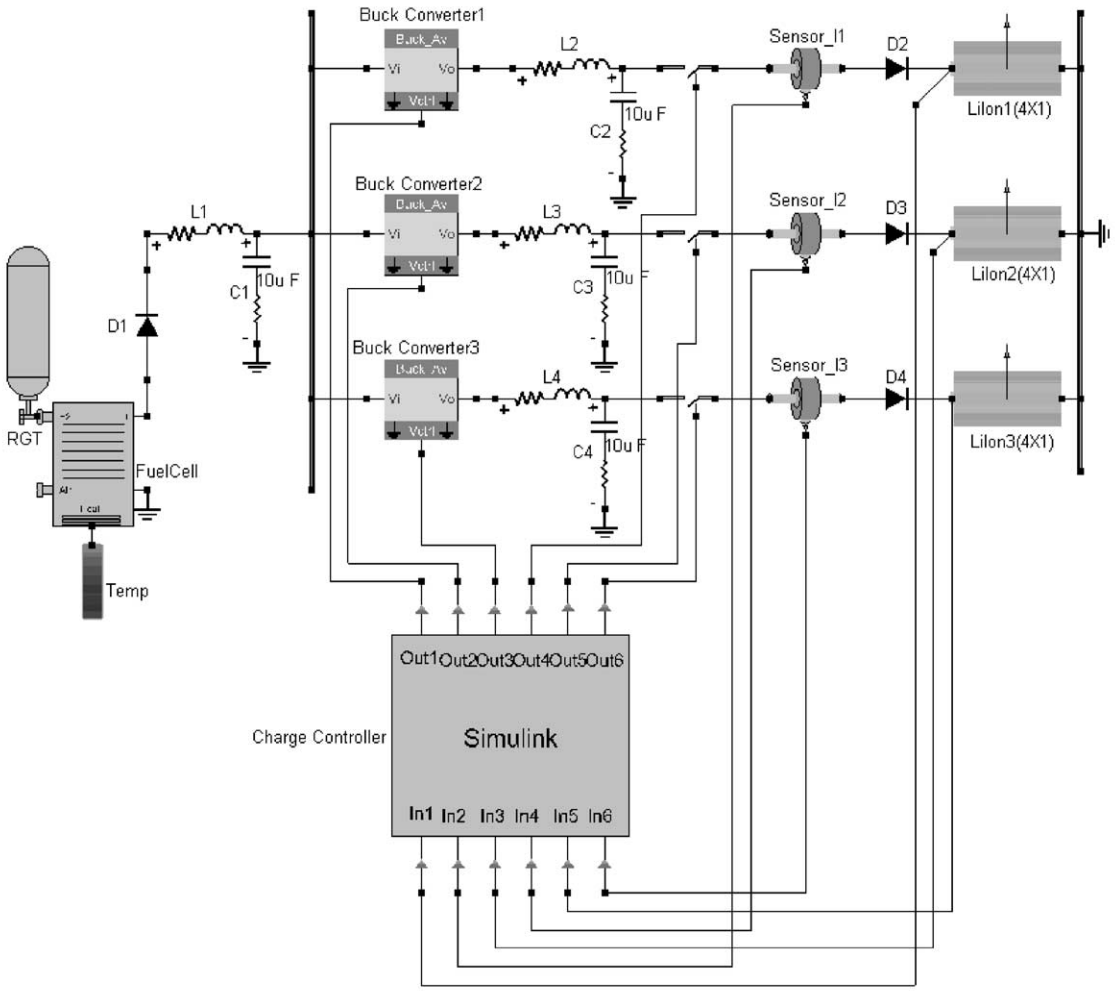

Fig. 7. Schematic view of the proposed fuel-cell powered battery charging station.

charging algorithms. Fig. 7 shows the VTB schematic view of the system shown in Fig. 1. The VTB model for the system consists mainly of a PEM fuel cell system, three buck converters, three lithium ion batteries, and a charge controller. The primary component of the fuel cell system is a fuel cell stack. The cell number is 25 and the nominal open-circuit voltage is 25.0 V. A hydrogen tank is connected to the stack to supply hydrogen for the fuel cell. The thermal source is used to exchange the heat of the fuel cell stack with the ambient. Assume here that the air is sufficient and that the air consumed by the fuel cell is not regulated. The fuel cell stack is connected to the power bus through a low-pass filter. The power circuit for each charging channel consists of an average-value buck converter model and a low-pass filter. Each battery is an array of 4×1 (series by parallel connections) lithium ion cells and is charged by an individual power converter. For convenience of demonstration, the batteries are numbered #1–3. The initial states of charge of batteries #1–3 are 0.60, 0.50, and 0.40, respectively. The power diodes are used to prevent the power from flowing in the opposite direction. The charge controller is implemented in the Simulink model as shown in Fig. 6, and imported to VTB for system simulation.

The conditions of the charging algorithms are explained as follows. The total available charging current for both equal rate charging algorithm and proportional rate charging algorithm is set to 2.0 A. The charging process stops when the charging current tapers below 0.1 A during constant voltage mode. The charging current of the pulse current charging algorithm is 1.4 A. The charging process stops when the battery voltage exceeds the reference voltage during low-value interval of the pulse. The simulated charging currents and states of charge of the batteries under these three charging algorithms are shown in Fig. 8a–f, respectively.

As shown in Fig. 8a, with the equal rate charging algorithm, each battery is charged at the same current with the magnitude of 0.67 A. It is seen that battery #1 needs about 70 min to become full. The charging time of battery #1 under this algorithm is the shortest among three algorithms, as shown in Fig. 8. It takes 100 min for battery #3 to be fully charged. The charging time of battery #3 is the longest among these algorithms.

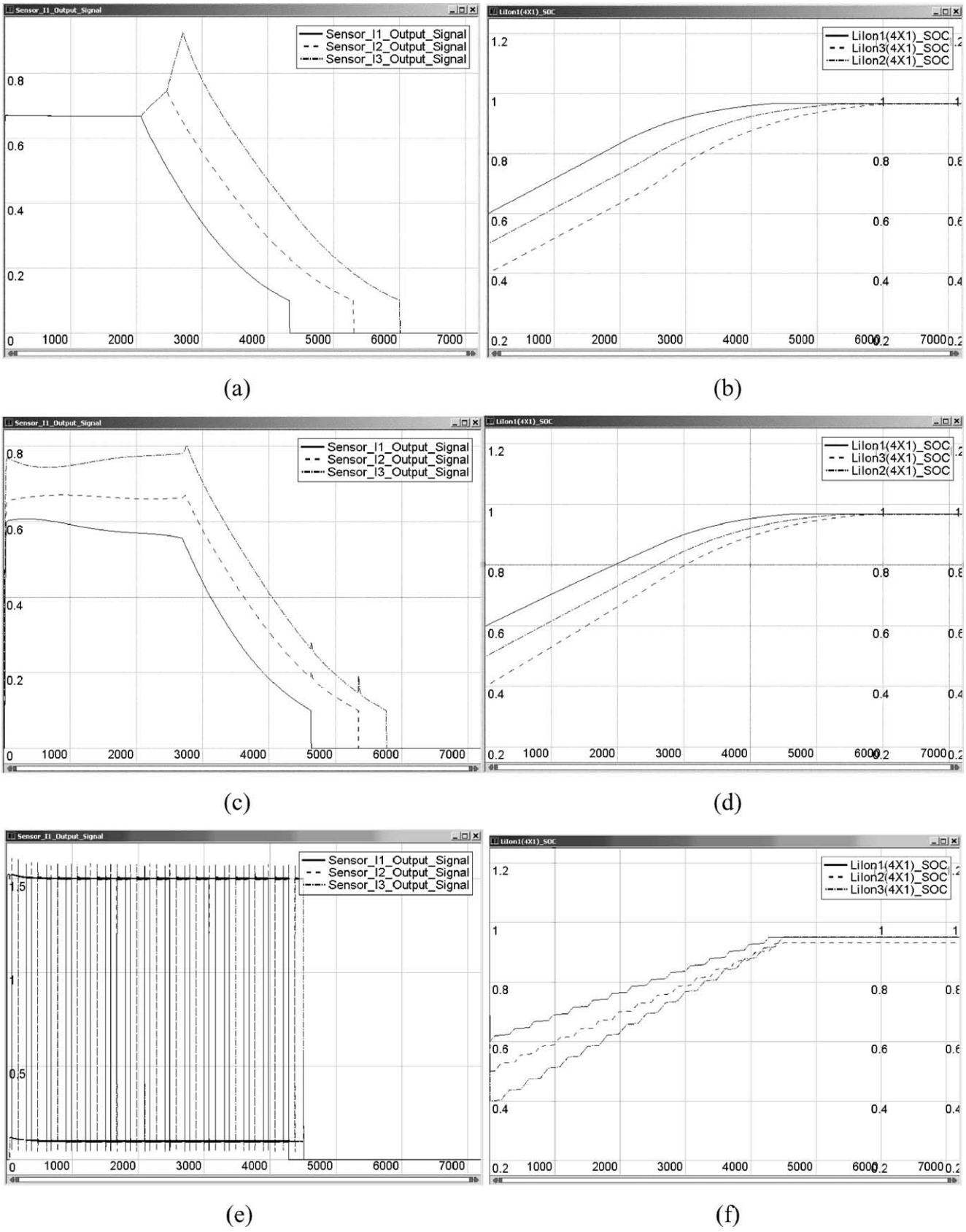

Fig. 8. Simulation results under three charging algorithms. (a–b) Equal rate charging; (c–d) proportional rate charging; (e–f) pulse current charging.

In Fig. 8c, it is shown that the charging current of each battery varies with the battery voltage and thus with the estimated SOC under the proportional rate charging algorithm. The battery with the lowest SOC is charged at the highest rate. It is clear that all the batteries reach the constant voltage mode almost simultaneously. The charging times of three batteries are 78, 88, and 96 min, respectively.

With the pulse current charging algorithm, the duty cycle of each pulse current also varies with the estimated SOC, as shown in Fig. 8e. The battery with the lowest SOC is charged by a pulse current with the largest duty cycle. Fig. 8e also shows that all the batteries become full almost simultaneously. The charging time for all batteries to be fully charged is 75 min, which is the shortest among three algorithms.

From the simulation results, the following conclusions can be drawn for the proposed three charging algorithms:

(1) The equal rate charging algorithm requires the shortest charging time for the battery with the highest initial SOC but the longest charging time for the battery with the lowest initial SOC among these algorithms.
(2) All the batteries can move to the constant voltage mode almost simultaneously with the proportional rate charging algorithm.
(3) All the batteries can become full almost simultaneously with pulse current charging algorithm. The charging time for all the batteries to be fully charged with this algorithm is the minimum among these algorithms.

6. Conclusions

This paper presents an approach to the design and testing of a fuel-cell powered battery charging station using the Virtual Test Bed. In this paper, the system design is first proposed. Both static and real-time control strategies are investigated to coordinate the power distribution among batteries. Interdisciplinary models such as the fuel cell and battery system and the model of the power converter are developed natively in VTB. The control system is modeled in MatLab/Simulink and then imported into VTB. Based on the native and imported models, the fuel-cell powered battery charging station is simulated under the proposed charging algorithms. The performance of each charging algorithm is analyzed.

The following conclusions were drawn for the proposed three charging algorithms. The equal rate charging algorithm has the minimum charging time for the battery with the highest initial SOC but the longest charging time for the battery with the lowest initial SOC among these algorithms. It is easiest to implement this algorithm in practical controller hardware. With proportional rate charging algorithm, all the batteries can move to the constant voltage mode almost simultaneously. The pulse current charging algorithm requires the minimum charging time for all the batteries but the algorithm is most difficult to implement.

From the studies in this paper, it can be seen that the VTB is an effective computational environment for virtual-prototyping multidisciplinary systems and studying the dynamic performances of complex systems.

Acknowledgements

This work was supported by the US Army CECOM and the NRO under contract NRO-00-C-0134, and US ONR under contract N00014-00-1-0368.

References

[1] R.J. Brodd, Overview: rechargeable battery systems, in: Proceedings of the WESCON'93 Conference, 1993, pp. 206–209.
[2] B. Rohland, J. Nitsch, H. Wendt, Hydrogen and fuel cells—the clean energy system, J. Power Sources 37 (1/2) (1992) 271–277.
[3] A. Heinzel, C. Hebling, M. Müller, M. Zedda, C. Müller, Fuel cells for low power applications, J. Power Sources 105 (2) (2002) 148–153.
[4] Z. Jiang, R.A. Dougal, Control design and testing of a novel fuel-cell powered battery charging station, in: Proceedings of IEEE Applied Power Electronics Conference, Miami, FL, 9–13 February 2003.
[5] M.M. Bernardi, M.W. Verbrugge, A mathematical model of the solid-polymer-electrolyte fuel cell, J. Electrochem. Soc. 139 (9) (1992) 2477–2491.
[6] J. Kim, S.-M. Lee, S. Srinivasan, Modeling of proton exchange membrane fuel cell performance with an empirical equation, J. Electrochem. Soc. 142 (8) (1995) 2670–2674.
[7] L. Song, J.W. Evans, Electrochemical–thermal model of lithium polymer batteries, J. Electrochem. Soc. 147 (6) (2000) 2086–2095.
[8] J. Li, E. Murphy, J. Winnick, P.A. Kohl, The effects of pulse charging on cycling characteristics of commercial lithium-ion batteries, J. Power Sources 102 (1/2) (2001) 302–309.
[9] R.A. Dougal, T. Lovett, A. Monti, E. Santi, A multilanguage environment for interactive simulation and development of controls for power electronics, in: Proceedings of the IEEE Power Electronics Specialists Conference, Vancouver, Canada, 17–22 June 2001.
[10] Z. Jiang, R.A. Dougal, Design, rapid prototyping, and testing of a portable fuel-cell powered battery charging station, in: Proceedings of the IEEE Power Electronics Specialist Conference, Acapulco, Mexico, 2003.
[11] D.A. Calahan, Computer-Aided Network Design, revised ed., McGraw-Hill, New York, 1972.
[12] G. Squadrito, G. Maggio, E. Passalacqua, F. Lufrano, A. Patti, An empirical equation for polymer electrolyte fuel cell (PEFC) behavior, J. Appl. Electrochem. 29 (1999) 1449–1455.
[13] L. Gao, S. Liu, R.A. Dougal, Dynamic lithium-ion battery model for system simulation, IEEE Transactions on Components and Packaging, in press.
[14] D. Bernardi, E. Pawlikowski, J. Newman, A general energy balance for battery systems, J. Electrochem. Soc. 132 (1) (1985) 5–12.